Permeation of Gases Across the Poly(chloro-*p*-xylylene) Membrane

AKIHIKO TANIOKA,[1,*] NORIAKI FUKUSHIMA,[1] KOICHI HASEGAWA,[1] KEIZO MIYASAKA,[1] and NOBORU TAKAHASHI[2]

[1]Department of Organic and Polymeric Materials, Tokyo Institute of Technology, Ookayama, Meguro-ku, Tokyo 152, Japan; [2]Research Center, Sony Corporation, 174 Fujitsuka-cho, Hodogaya-ku, Yokohama 240, Japan

SYNOPSIS

Gas permeabilities across poly(chloro-*p*-xylylene) (parylene C) films are measured with different thicknesses of 20.2, 10.0, 8.9, 4.6, 3.4, and 1.0 μm. Measurements were carried out below 1 atm and between 10 and 80°C, which are under the glass transition temperature. The temperature and pressure dependencies of the permeability and the apparent diffusion coefficients were measured. If the membrane thickness is larger than 8 μm, the gas-transport mechanism is solution–diffusion, which implies that it is pinhole-free, because the pressure dependency of the permeability cannot be found and the apparent activation energy of permeation and diffusion are observed. If the membrane thickness is less than 8 μm, the gas transport mechanism is pore flow combined with solution–diffusion flow because gas may penetrate both the porous area and the polymer matrix. The thinner the membrane, the higher is the permeability coefficient, since the diameter and number of pores increase with decrease of the membrane thickness. The gas permeability coefficient has different values at the same pressure or temperature. As this film is in the glassy state, it should be explained using the average ordering parameter (ξ), which is a function of temperature, pressure, gas concentration, and time. © 1994 John Wiley & Sons, Inc.

INTRODUCTION

Poly(chloro-*p*-xylylene) (parylene C) films show extremely high resistance to gas- or water-vapor penetration[1-3] and have been used in many commercial applications, such as dielectric coatings and encapsulation of semiconductor devices.[4] The thin layer less than a few micrometers can be polymerized directly and uniformly on a base material, which is called the vacuum-deposition polymerization method.

The thickness of the coated layer is controlled by varing the deposition time. It has been suggested that there is a distinction in the physical property between the thicker layer and the thinner one. That is caused by the membrane structure difference in the amorphous polymer region, which is dependent on the thickness. However, such a structure cannot be clarified by electron microscopy, X-ray diffraction, or infrared spectroscopy. Measurement of gas permeability is one of the methods to elucidate the amorphous structure of parylene C.

The permeability coefficients (P) are functions of both temperature and applied pressure. If a membrane is homogeneous and dense, the permeability coefficient is constant in the range where plasticization by gas solubility or compaction by pressure is ignored, and the logarithmic permeability coefficient is proportional to the reciprocal absolute temperature ($1/T$) with a negative slope[5,6]:

$$P = \text{const at ranging pressure} \quad (1)$$

$$\ln P = \ln P_0 - E_P/RT \quad (2)$$

where P_0 is the preexponential permeability; E_P, the apparent activation energy of permeability; and R, the gas constant. If the membrane is porous, two different kinds of flow, which are called viscous and Knudsen flows, are observed.[7,8] In the case of the

* To whom correspondence should be addressed.

Journal of Applied Polymer Science, Vol. 54, 219–229 (1994)
 CCC 0021-8995/94/020219-11

viscous flow where the pore diameter d is much larger than the mean free path of the gas λ ($d \gg \lambda$), the permeability coefficient is increased with pressure and proportional to the reciprocal absolute temperature:

$$P = (B/\eta)(p_1 + p_2)/2 \quad (3)$$

$$P = (A_1/\eta)/T \quad (4)$$

where p_1 and p_2 are the gas pressures at both sides of a membrane; η, the viscosity of gas; and B (> 0) and A_1 (> 0) are the parameters that are characteristic to the membrane. In case of the Knudsen flow ($d \ll \lambda$), the permeability coefficient is constant at the ranging pressure and proportional to the square root of reciprocal absolute temperature and gas molecular weight M:

$$P = \text{const at ranging pressure} \quad (5)$$

$$P = (A_2/M^{1/2})(1/T^{1/2}) \quad (6)$$

where A_2 (> 0) is the parameter that is characteristic to the membrane. If a homogeneous dense membrane includes pinholes in itself, as shown in Figure 1, the permeability coefficient shows a minimum with respect to the temperature change[9-12]:

$$P = P_0^0 \exp(-E_P/RT) + A'/T \quad (7)$$

$$P = P_0^0 \exp(-E_P/RT) + A''/T^{1/2} \quad (8)$$

where P_0^0 is the preexponential factor and A' (> 0) and A'' (> 0) are the parameters that are characteristic to the membrane.

If temperature, pressure, and gas molecular weight dependencies of the permeability coefficients are investigated, the membrane structure has to be understood more precisely.[13] It is so important to clarify the relationship between the gas permeability and the structure of the thin membrane in order to give instructions for the development of not only a good gas barrier material but also of an active thin layer in the composite gas-separation membrane.

EXPERIMENTAL

Materials

Poly(chloro-*p*-xylylene) membranes were prepared using a vacuum-deposition method (Union Carbide Corp.). Prior to the fabrication of poly(chloro-*p*-xylylene) films, the dimer (dichloro[2,2]paracyclophane) was placed in an air-tight container made of glass and vaporized at a pressure of 8×10^{-3} mmHg at 140–170°C before decomposing to a monomer at about 700°C. The vaporized monomer is deposited and polymerized on the glass plate at about 25°C. The processes cited above are performed continuously, which is called the vacuum-deposition method. The thickness of the membrane is controlled by the depositing time. Various kinds of sample, which have different thicknesses of 20.2, 10.0, 8.9, 4.6, 3.4, and 1.0 μm, were prepared. The film was peeled off from the base glass plate to use in the following experiments. The glass transition and melting point temperatures were reported to be 80–100°C and 290°C, respectively. Crystallinity was measured using an X-ray diffractometer to be resolved as 20–50%.

Measurements of Permeability and Apparent Diffusion Coefficients

Permeability and apparent diffusion coefficients were measured by using a high-vacuum method. After both sides of a membrane were evacuated, gas was introduced into one side of the membrane. Pressure of the permeated gas from the high- to low-

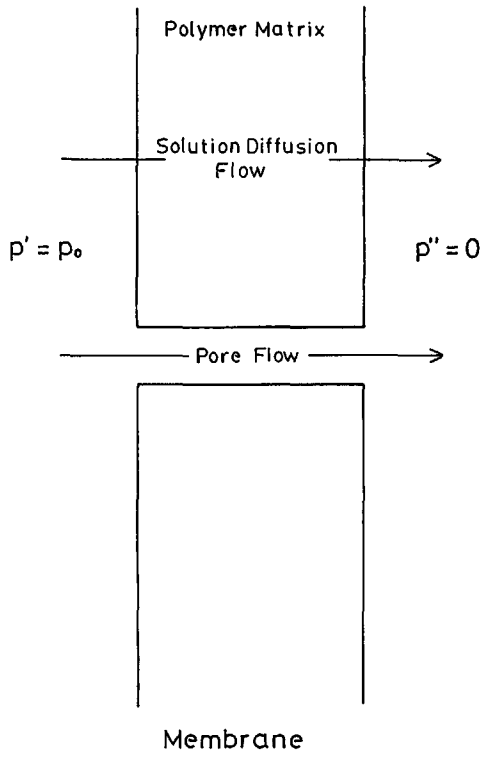

Figure 1 Schematic diagram of inhomogeneous polymer membrane.

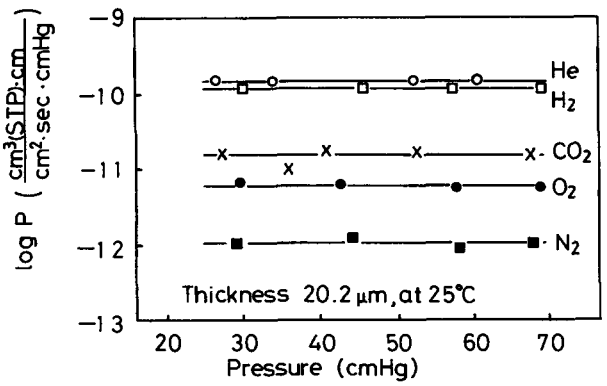

Figure 2 Permeability coefficients of He, H_2, CO_2, O_2, and N_2 gases as a function of pressure at 25°C for the 20.2 μm membrane.

pressure side was measured as a function of time using a differential pressure gauge of the diaphragm type (Baratron 310 BH-10). The relationship between time and gas pressure is convexed to time axis at the earlier stage of time and then becomes a linear line if the steady state is attained. The gas pressure in the low-pressure side was always maintained at less than one hundredth of that in the high-pressure side to keep a linear line at the steady state. The permeability coefficient was calculated from the slope of a linear line at the steady state. The apparent diffusion coefficient was also calculated using a time lag that was obtained from the intersecting point of the time axis with an extrapolating line of the slope at the steady state. These measurements were done below 1 atm and at 10–80°C. H_2, He, CH_4, N_2, O_2, and CO_2 gases were used.

RESULTS AND DISCUSSION

In Figure 2, the gas permeability coefficients (P) through a membrane, where the sample thickness is 20.2 μm (abbreviated as the 20.2 μm membrane), are plotted as a function of applied pressure on the high-pressure side of the membrane for He, H_2, CO_2, O_2, and N_2 gases. The P were kept constant as the applied pressure varied, which implied that the transport mechanism was not a viscous flow, but a solution–diffusion or a Knudsen (molecular) one. The P are not a function of the reciprocal square root of the gas molecular weight. This is evidence of the fact that the transport mechanism is not a Knudsen flow. In Figure 3, the logarithmic permeability coefficients for different gases through the 20.2 μm membrane are plotted against the reciprocal absolute temperature. A good linear relationship is obtained for them. Therefore, these results show that the gas transport is controlled by a solution–diffusion mechanism. The permeability coefficients are not lined up in the order of the gas diameter, because they are not affected only by the solubility, but also by the diffusivity, where the permeability coefficient (P) is equal to the diffusion coefficient (D) times the solubility coefficient (S)[5,6]:

$$P = DS \tag{9}$$

From the relationship between the logarithmic permeability and the reciprocal absolute temperature, the apparent activation energy of permeation is calculated and shown in Table I for 10.0 and 20.2 μm membranes. It is very difficult to find the difference between the 10.0 and 20.2 μm membranes.

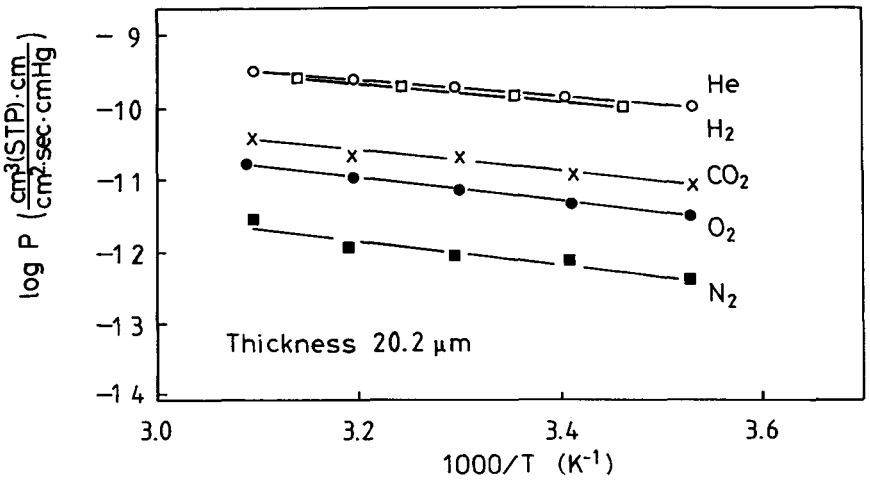

Figure 3 Permeability coefficients of He, H_2, CO_2, O_2, and N_2 gases as a function of reciprocal absolute temperature for the 20.2 μm membrane.

Table I Apparent Activation Energies of Permeation and Diffusion and Enthalpy of Solution for He, H_2, CO_2, O_2, and N_2 gases in 10.0 and 20.2 μm Membranes

	E_p (kJ/mol)		E_D (kJ/mol)		ΔH (kJ/mol)	
	Thickness					
Gas	10.0 μm	20.2 μm	10.0 μm	20.2 μm	10.0 μm	20.2 μm
He	21.7	21.6	14.6	28.3	7.1	−6.7
H_2	24.1	22.8	18.5	35.9	5.6	−13.1
CO_2	27.8	27.0	51.3	61.9	−23.4	−34.9
O_2	29.5	30.4	32.5	50.8	−3.0	−20.4
N_2	31.3	30.9	30.1	59	1.2	−28.1

By calculating the permeability coefficient ratios of each gas to the N_2 gas for the 20.2 μm membrane, $He/N_2 = 225$, $H_2/N_2 = 114$, $CO_2/N_2 = 17$, and $O_2/N_2 = 5.7$. These values show that parylene C can possibly be used as a gas-separation membrane.

In Figure 4, the logarithmic apparent diffusion coefficients of gases for the 20.2 μm membrane are plotted against the reciprocal absolute temperature. Good linear relationships are obtained for them and the apparent activation energy of diffusion (E_D) can be calculated. E_D's are shown in Table I for each gas with the results of 10.0 μm membrane. The E_D for the 10.0 μm membrane is smaller than that for the 20.2 μm one. The lower the activation energy is, the easier the gas molecules can diffuse. In Table II, the permeability, apparent diffusion, and solubility coefficients of various gases at 25°C are shown for the 10.0 and 20.2 μm membranes. The permeability and the apparent diffusion coefficients of the thinner membrane are smaller than those of the thicker one. This evidence introduces the geometric impediment parameter τ, which is called the tortuosity factor[5,6]:

$$D = D_a \varepsilon / \tau \tag{10}$$

where D_a are the diffusion coefficients of the amorphous phase of the polymer, and ε, the amorphous volume fraction. If the crystallinity or ordered part of this polymer, where a gas molecule cannot penetrate easily, is increased, ε decreases and τ increases. Since D_a is considered to be constant, D should be decreased by ε and τ. The gas transport mechanism through the polymer film has been explained by the free-volume or molecular theory. In Figure 5, the apparent activation energy of diffusion is shown as a function of the molecular diameter of the gas. The apparent activation energy of diffusion increases with increasing of the molecular diameter of the gas. Pace and Datyner predicted the activation energy of diffusion as a function of the gas molecular di-

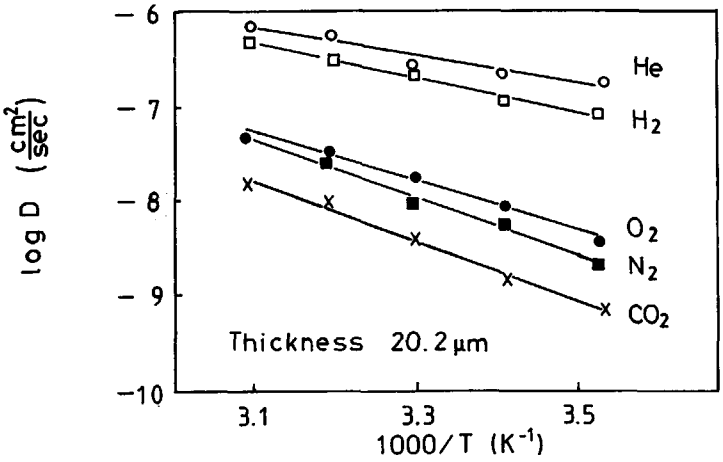

Figure 4 Apparent diffusion coefficients of He, H_2, CO_2, O_2, and N_2 gases as a function of reciprocal absolute temperature for the 20.2 μm membrane.

Table II Permeability, Apparent Diffusion, and Solubility Coefficients of He, H_2, CO_2, O_2, and N_2 gases for the 10.0 and 20.2 μm Membranes at 25°C

	$P \times 10^{10}$ $\frac{cm^3\ (STP)\ cm}{cm^2\ s\ cmHg}$		$D \times 10^7$ $\frac{cm^2}{s}$		$S \times 10^3$ $\frac{cm^3\ (STP)}{cm^3\ cmHg}$	
	Thickness					
Gas	10.0 μm	20.2 μm	10.0 μm	20.2 μm	10.0 μm	20.2 μm
He	1.88	1.52	1.03	2.92	1.83	0.521
H_2	0.956	1.33	0.675	1.49	1.42	0.893
CO_2	0.140	0.159	0.0164	0.0258	8.54	6.16
O_2	0.0477	0.0622	0.0351	0.0823	1.36	0.756
N_2	0.00835	0.0109	0.0178	0.0947	0.469	0.115

ameter from the viewpoint of the molecular theory.[14–16] In several cases, some drafts of the gas molecular diameter can introduce a good correlation between them. In Figure 5, the 20.2 μm membrane shows a good linear relationship without drafts of the gas molecular diameter. On the other hand, it seems to be convex to the abscissa and gives some drafts of the gas molecular diameters to give a good correlation for the thinner one. The activation of energy of diffusion is also explained from the free-volume theory using the following equation[5]:

$$\Delta E_d = (\pi/4)d^2\lambda\ (CED) \qquad (11)$$

where d is the diameter of the gas molecule; λ, the length of a diffusional step; and CED, the cohesive energy density. If $(\pi/4)d^2\lambda$ is equal to the free volume of the polymer that is produced by one jump of the polymer motion $(Q_{00} - V_{00})$, a gas molecule can jump from one "hole" to a different "hole" as shown in eq. (12):

$$Q_{00} - V_{00} = (\pi/4)d^2\lambda \qquad (12)$$

In Figure 6, the apparent activation energy of diffusion is plotted as a function of $(Q_{00} - V_{00})$. If the diffusion mechanism obeys to the free-volume theory, the relationship cited above should be linear. However, we cannot find any linear relationship between them, which suggests that the theory is not applied to the system of parylene C and gases. It, however, is very difficult to decide the diffusion mechanism from only these data.

It was impossible to decide the apparent diffusion coefficient for the membranes whose thicknesses were less than 8 μm because time lag could not be observed in the permeation measurement. In Figure 7, the permeability coefficients of N_2, O_2, and CO_2

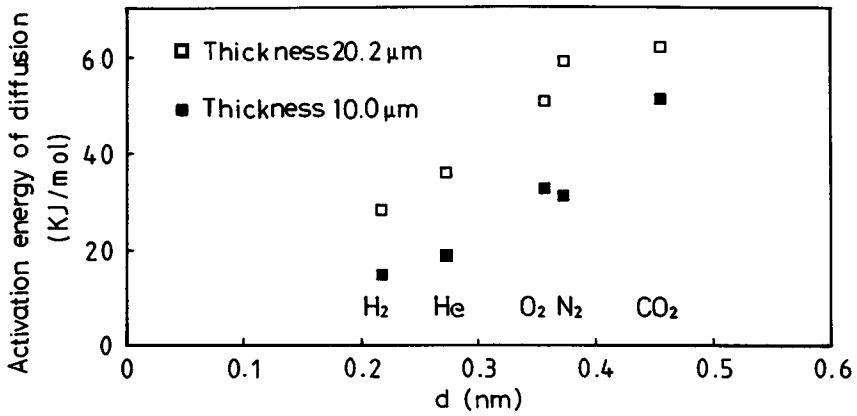

Figure 5 Apparent activation energies of diffusion for He, H_2, CO_2, O_2, and N_2 gases as a function of gas molecular diameter for the 10.0 and 20.2 μm membranes.

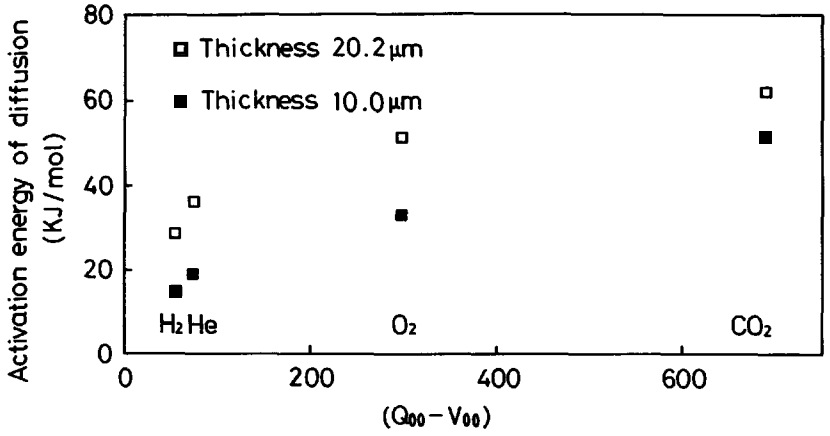

Figure 6 Apparent activation energies of diffusion for He, H_2, CO_2, O_2, and N_2 gases as a function of free volume for the 10.0 and 20.2 μm membranes.

gases through the 4.6 μm membrane are plotted as a function of pressure in the high-pressure side. Squares, triangles, and circles show O_2, N_2, and CO_2 gases, respectively. Solid symbols mean that the measurement series was carried out by changing the pressure in the high-pressure side from high to low, which is shown as "down," and open symbols, from low to high pressure, shown as "up." Permeability coefficients increase with pressure increase and their intersections are not 0 at $p = 0$, which suggests that the pore flow coexisted with the diffusive flow.[9,10] In Figure 8, permeability coefficients of N_2, O_2, and CO_2 gases through 4.6 μm are plotted as a function of reciprocal temperature where the cross, solid circle, and solid square are CO_2, O_2, and N_2, respectively. In the higher-temperature region, permeability coefficients decrease with increase of the reciprocal absolute temperature ($1/T$), and in the lower-temperature region, increase with increase in $1/T$. If the gas permeation is controlled by the solution–diffusion mechanism, logarithmic permeability decreases with increase in $1/T$. On the other hand, the permeability coefficient increases with increase in $1/T$ in the case of the pore flow. If both flows are coexisting, the permeability coefficient is able to show the minimum with respect to the temperature change as shown in eqs. (7) and (8).[12] Therefore, the minima in Figure 8 suggest that gases penetrate both amorphous polymer regions and pinholes simultaneously for the 4.6 μm membrane. In the lower $1/T$, the permeability coefficients of CO_2 are the largest and those of O_2 and N_2 are similar

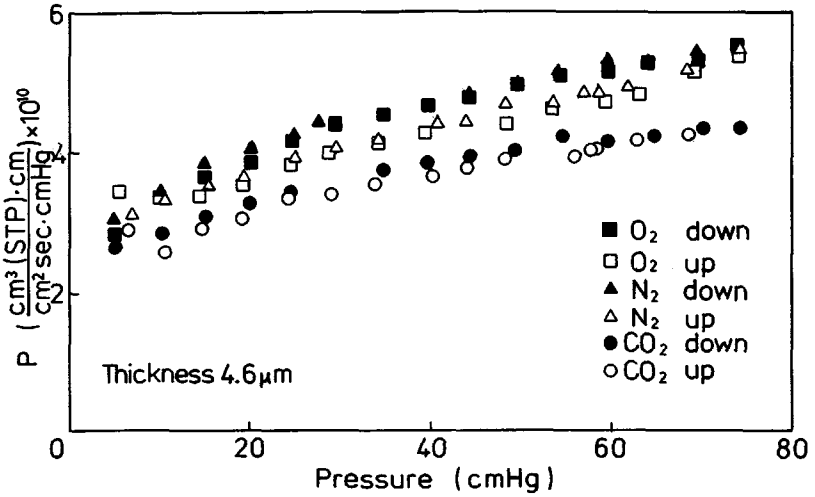

Figure 7 Permeability coefficients of O_2, N_2, and CO_2 gases as a function of pressure for the 4.6 μm membrane. Solid symbols show that the measurements were made by changing the pressure from high to low, and open symbols, from low to high.

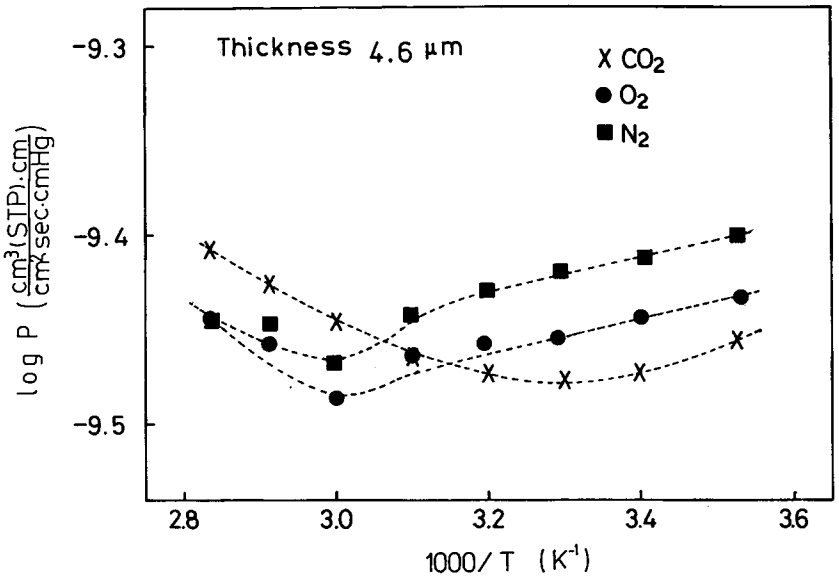

Figure 8 Permeability coefficients of O_2, N_2, and CO_2 gases as a function of reciprocal absolute temperature for the 4.6 μm membrane.

to each other, which corresponds to the solution-diffusion mechanism. On the other hand, permeability coefficients of CO_2, O_2, and N_2 are in the order of molecular weight at the higher $1/T$, which implies the pore flow. In Figure 7, the permeability coefficients of the "down" process are larger than those of the "up" process. Such a difference shows that the permeability coefficient has various values at the same pressure.

In Figure 9, N_2 permeability coefficients of the 3.4 μm membrane, which were measured four times, are plotted as a function of pressure in the chamber of the high-pressure side. The first curve, which is shown as open circles, was measured by changing from low to high pressure at the high-pressure side, where the permeability coefficient increases with increase in pressure in the lower-pressure side and decreases with increase in pressure in the higher-pressure side. The second curve, which is shown by open triangles, was measured by changing the pressure from high to low after the measurement of the first step, where the permeability coefficient has a minimum and a maximum. The third curve, which is shown by open squares, was measured in the same way as the first step. The permeability coefficient increases with increase in pressure in the lower-pressure side and after that becomes nearly constant. The fourth curve, which is shown by open hexagons, was measured by the same way as was the second step after the measurement of third step, where the permeability coefficient increases with increase in pressure at the lower-pressure and decreases with increase in pressure at the higher-pressure.

These permeability curves show that the permeability coefficients through the 3.4 μm membrane have different values at the same pressure. The same tendency is observed for the O_2 gas. In Figure 10, the permeability coefficients of CO_2 gas are plotted as a function of the applied pressure at the high-pressure side. The experimental procedure is the same as for N_2 and O_2. From the first to third step, the permeability coefficient changes greatly, but from the third to fourth step, we cannot find a big difference. It is supposed that CO_2 is easy to use to plasticize the polymer to attain the final stable state by repeating the measurement.[17-20] In Figure 11, the permeability coefficients of CO_2, N_2, and O_2 through the 3.4 μm membrane are plotted as a function of reciprocal temperature. The measurement was done in the order of CO_2, N_2, and O_2 gases. Dotted lines are the first steps of measurement and solid lines are the final steps for each gas. Every permeability coefficient increased with increase in pressure and was in the order of molecular weight at the final step, which implies that the pore flow is predominant. The large shift of the permeability coefficient of N_2 between low and high temperature means that the membrane structure was affected by the temperature change.

In Figure 12, the permeability coefficients of N_2 gas for the 1.0 μm membrane are plotted as a function of pressure in the chamber of the high-pressure

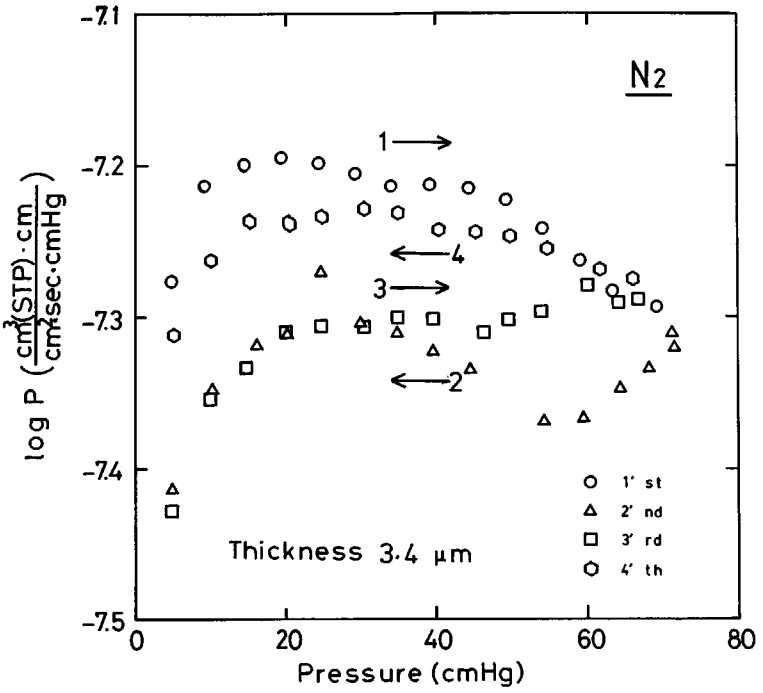

Figure 9 Permeability coefficients of the N_2 gas as a function of pressure for the 3.4 μm membrane. The circle indicates that the measurement was performed from low to high pressure as the first step; the triangle, from high to low as the second; the square, from low to high as the third; and the hexagonal, from high to low as the fourth.

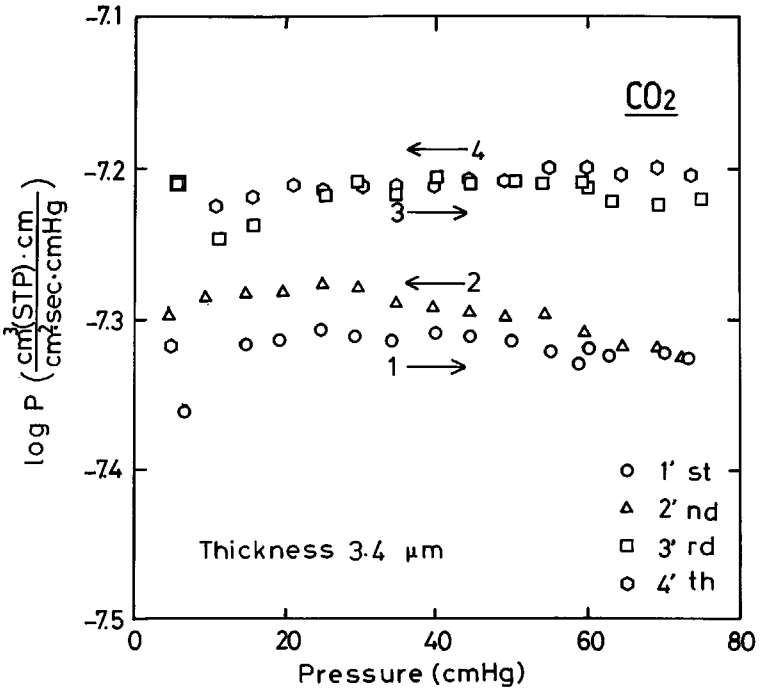

Figure 10 Permeability coefficients of the CO_2 gas as a function of pressure for 3.4 μm membrane. The circle indicates that the measurement was performed from low to high pressure as the first step; the triangle, from high to low as the second; the square, from low to high as the third; and the hexagonal, from high to low as the fourth.

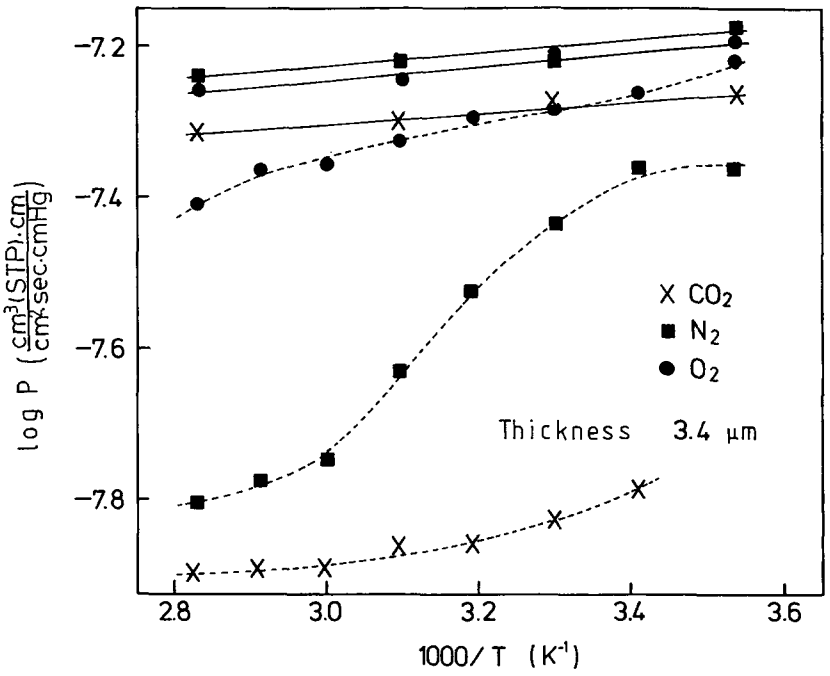

Figure 11 Permeability coefficients of O_2, N_2, and CO_2 gases as a function of reciprocal absolute temperature for the 3.4 μm membrane. The dotted line shows the first step of measurement, and the solid one, the final step.

side. Open circles show that the measurement series was made from low to high pressure at the high-pressure side. Solid circles show that the measurement was done from high to low pressure. At the lower pressure, the permeability coefficients of "down" and "up" processes show different values at the same pressure. A similar result was observed for O_2 gas. Such variation of the permeability coefficient means that the membrane structure changes by pressure. On the other hand, the permeability coefficients do not change very much with both processes in the case of CO_2 gas. In Figure 13, the permeability

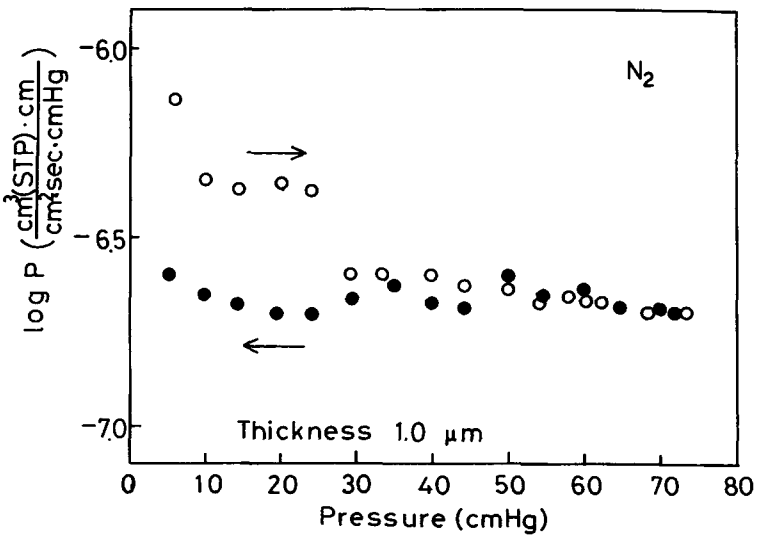

Figure 12 Permeability coefficients of the N_2 gas as a function of pressure for the 1.0 μm membrane. The open circle indicates that the measurement was performed from low to high pressure, and the solid circle, from high to low.

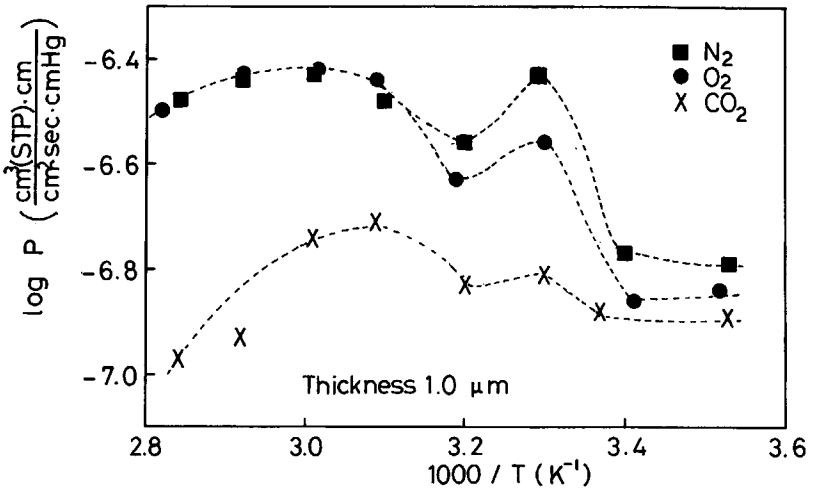

Figure 13 Permeability coefficients of O_2, N_2, and CO_2 gases as a function of reciprocal absolute temperature for the 1.0 μm membrane.

coefficients of N_2, O_2, and CO_2 are plotted as a function of the reciprocal absolute temperature. The permeability coefficients are very sensitive to the temperature, which implies that the membrane structures are varying with temperature change, so that an appropriate transport mechanism cannot be predicted. In the lower $1/T$ (the higher temperature), the permeability coefficients of N_2 are the same as those of O_2 and larger than those of CO_2, and all of them increase with increase in $1/T$, which suggests that the pore flow is predominant in this temperature range. On the other hand, the permeability coefficient difference between N_2 and CO_2 becomes small, and O_2 permeability is located between N_2 and CO_2 at the higher $1/T$ (the lower temperature). These results suggest that pore flow is predominant in the higher temperature, and solution–diffusion flow, in the lower temperature. It is explicitly different from the results of the 4.6 and 3.4 μm membranes.

In Figure 14, the permeability coefficients of CO_2 gas at 25°C and 32 cmHg are plotted as a function of membrane thickness. If the membrane thickness is larger than 8 μm, the permeability coefficients are independent of it, where the membrane is pinhole-free. On the other hand, the permeability coefficient increases with decrease in membrane thickness because of the pinhole formation if it is less than 8 μm. It has been already pointed out, vaguely, that the physical property has a certain kind of distinction between the thicker layer and the thinner one. It was very difficult to determine the structure differences among them by means of an electromicroscope or X-ray diffraction. However, the gas permeability measurement can indicate clearly such a difference.

Results from Figures 9–12 suggest that there exist different permeabilities at one temperature or at one pressure. Yasuda et al. showed that the relationship between the permeability coefficient and the membrane crystallinity cannot be found, so that the structure of the amorphous region in the polymer membrane is very effective in the permeability change.[3] The polymer chain is not distributed uniformly in the amorphous region of the glassy polymer. The heterogeneity of the chain distribution easily produces pinholes through the membrane if the thickness is very thin. Since the chain distribution strongly depends on the pressure and tem-

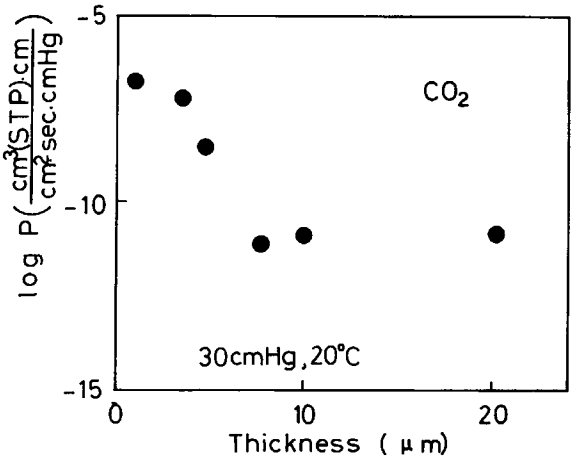

Figure 14 Permeability coefficient of the CO_2 gas as a function of membrane thickness.

perature, the permeability coefficient should be a function of not only pressure and temperature, but also a parameter of structure. Introduction of the ordering parameter (ξ), which corresponds to the degree of the reaction (or extent of change) based on nonequilibrium thermodynamics, can explain the state of glassy polymer exactly.[21,22] Therefore, the permeability coefficient is a function of temperature (T), pressure (p), concentration of gas in the polymer (C_g), and the average ordering parameter (ξ) as shown in eq. (9)[23-25]:

$$P = \{ T, p, C_g, \xi(T, p, C_g, t) \} \qquad (13)$$

where the ordering parameter is also a function of T, p, C_g, and time (t). In the amorphous glassy polymer, each local region has a different kind of order, which are shown as ξ_1, ξ_2, $\cdots$ ξ_n. The gas molecule penetrates each part and the permeability coefficient is evaluated as a function of the average ordering parameter. Polymer chains change their positions by applying pressure, varing temperature, and gas sorption. The arrival state due to one of their processes depends not only on the former state, but also on the experimental procedures that imply time dependence, i.e., how to introduce gases to the chamber and absorb gases by the polymer and so on, because the polymer is in the nonequilibrium state. A difference of the polymer state is directly reflected by the ordering parameter. Therefore, the different permeability coefficients at the same pressure or temperature can be explained using the ordering parameter.

REFERENCES

1. M. A. Spivack and G. Ferrante, *J. Electrochem. Soc.*, **116,** 1592 (1969).
2. W. H. Hubbell, Jr., H. Brandt, and Z. A. Munir, *J. Polym. Sci. Polym. Phys. Ed.*, **13,** 493 (1975).
3. Y.-S. Yeh, W. J. James, and H. Yasuda, *J. Polym. Sci. Part B Polym. Phys.*, **28,** 545 (1990).
4. W. F. Gorham and W. D. Niegisch, Eds., *Encyclopedia of Polymer Science & Technology,* Wiley, New York, 1971, Vol. 15, p. 98.
5. J. Crank and G. S. Park, *Diffusion in Polymers,* Academic Press, London, 1968.
6. J. H. Petropoulos, *Advances in Polymer Science,* Springer, Berlin, 1979, Vol. 64.
7. P. G. Carman, *Flow of Gases Through Porous Media,* Butterworth, London, 1971.
8. H. Yasuda and J. T. Tsai, *J. Appl. Polym. Sci.*, **18,** 805 (1974).
9. H. L. Frisch, *J. Phys. Chem.*, **60,** 1177 (1956).
10. H. L. Frisch, *J. Phys. Chem.*, **61,** 93 (1957).
11. J. Crank, *The Mathematics of Diffusion,* 2nd ed., Oxford University Press, Oxford, 1975.
12. A. Tanioka, *Bull. Inst. Chem. Res. Kyoto Univ.*, **70,** 178 (1992).
13. N. Choji, W. Pusch, M. Satoh, T.-M. Tak, and A. Tanioka, *Desalination,* **53,** 347 (1985).
14. R. J. Pace and A. Datyner, *J. Polym. Sci. Polym. Phys. Ed.*, **17,** 437 (1979).
15. R. J. Pace and A. Datyner, *J. Polym. Sci. Polym. Phys. Ed.*, **17,** 453 (1979).
16. R. J. Pace and A. Datyner, *J. Polym. Sci. Polym. Phys. Ed.*, **17,** 465 (1979).
17. T. E. Whyte, Jr., C. M. Yon, and E. H. Wagener, Eds., *Industrial Gas Separation,* ACS Symp. Ser. 223, American Chemical Society, Washington, DC, 1983.
18. W. J. Koros, *J. Polym. Sci. Polym. Phys. Ed.*, **23,** 1611 (1985).
19. J. S. Chiou, Y. Maeda, and D. R. Paul, *J. Appl. Polym. Sci.*, **30,** 4019 (1985).
20. Y. Kamiya, K. Mizoguchi, Y. Naito, and T. Hirose, *J. Polym. Sci. Part B Polym. Phys.*, **24,** 535 (1986).
21. I. Prigogine and R. Defay, *Chemical Thermodynamics,* Longmans Green, London, 1954.
22. R. N. Haward, *The Physics of Glassy Polymers,* Applied Science, London, 1973.
23. G. Astarita, M. E. Paulaitis, and R. G. Wissinger, *J. Polym. Sci. Polym. Phys. Ed.*, **27,** 2105 (1989).
24. S. Motamedian, W. Pusch, G. Sendelbach, T.-M. Tak, and A. Tanioka, in *Proceedings of ICOM 90,* 1990, Vol. 2, p. 341.
25. A. Tanioka and K. Miyasaka, in *Membrane Symposium,* 1990, No. 2, p. 64.

Received January 22, 1994
Accepted March 7, 1994